GEOLOGICA CARPATHICA, JUNE 2010, 61, 3, 211–225 doi: 10.2478/v10096-010-0012-5

Reconstruction of Cenozoic paleostress fields and revised tectonic history in the northern part of the Central Western Carpathians (the Spišská Magura and Východné Tatry Mountains)

RASTISLAV VOJTKO✉, EVA TOKÁROVÁ†, ĽUBOMÍR SLIVA and IVANA PEŠKOVÁ

Department of Geology and Paleontology, Faculty of Natural Sciences, Comenius University, Mlynská dolina G, 842 15 Bratislava, Slovak Republic; vojtko@fns.uniba.sk; sliva@fns.uniba.sk; peskova@fns.uniba.sk

(Manuscript received June 29, 2009; accepted in revised form December 11, 2009)

Abstract: This study investigates the chronology of paleostress evolution and faulting in the northern part of the Central Western Carpathians (Spišská Magura and Východné Tatry Mts). Paleostress analysis of brittle and semibrittle structures of the Eocene–Oligocene succession of the Central Carpathian Paleogene Basin (CCPB) supplemented by measurements in the Triassic sequence of the Krížna Nappe, revealed the existence of six tectonic regimes during the Cenozoic. Orientation of the paleostress field before the deposition of the CCPB was characterized by the E-W oriented compression. After this compression, the paleostress field rotated approximately 40–50°, and NW–SE directed compression took place in the Early Miocene. During the latest Early Miocene, the extensional tectonic regime with fluctuation of σ_3 orientation between NW-SE to NE-SW dominated. The Late Badenian–Pannonian is characterized by a new compressive to strike-slip tectonic regime during which the principal maximum stress axis σ_1 progressively rotated from a NW-SE to a NE-SW position. Uplift and tilting of the Tatra Massif took place during this stage. The neotectonic stage (Pliocene to Holocene) is characterized by extensional tectonic regime with the two directions of tension. The first one is oriented in the E-W direction and could be considered older and the second one, NNW-SSE tension is considered to be Late Pliocene to Quaternary in age. In general, orientation of the stress fields shows an apparent clockwise rotation from the Oligocene to Quaternary times. This general clockwise rotation of the Oligocene to Quaternary paleostress fields could be explained by both the effect of the counter-clockwise rotation of the ALCAPA microplate and by the regional stress field changes.

Key words: Central Western Carpathians, Spišská Magura Mts, Východné Tatry Mts, structural analysis, neotectonics, paleostress reconstruction, fault-slip data.

Introduction

The Spišská Magura Mts — are situated in the northern part of the Central Western Carpathians (CWC, Fig. 1). They are surrounded by the Východné Tatry Mts and Levočské vrchy Mts in the south, by the Pieniny Klippen Belt in the northeast and the Podhale Basin in the west. The studied area consists predominantly of the Eocene to lowermost Miocene sedimentary succession of the Central Carpathian Paleogene Basin (CCPB).

The tectonic evolution of the northern part of the Central Western Carpathians and its surroundings has been reconstructed using data from over 350 fault slips, 90 fold axes and 200 tension gashes. The collected data have been used to determine paleostress field orientation and evolution. The majority of studied outcrops are in the bedrock exposures along the Biela Voda, Javorinka and Biela rivers and their tributaries. Eocene to Oligocene rocks of the CCPB in this area are faulted, fractured and folded. Most fault surfaces contain one or more sets of striae produced during different deformation episodes. The superposition of striae was useful for the separation of faults into the homogeneous groups. The investigated area offers quite a good opportunity to study brittle deformation and to attempt the determination of the states of stress associated with the faulting and folding.

A normal dip-slip movement along fault zones of the mountain front and related folding of Paleogene sedimentary sequences during the Neogene was a common view of geologists in the last century (Gross 1973; Gross et al. 1980; Maheľ 1986). However, new research into the Cenozoic tectonics in the Central Western Carpathians pointed out the importance of strike-slip and oblique-slip faulting developed during transpressional and transtensional tectonic regimes. During these tectonic regimes, varied tectonic structures (faults, folds, extensional veins, stylolites etc.) have been recorded in the host rocks.

The purpose of this paper is (a) to describe the regional and local geological settings, fault-slip and fold measurements and determinations that were made, (b) to summarize the results of fault and fold measurements and their kinematic determinations, and (c) to present the results of dynamic analysis oriented predominantly to the paleostress field determination by a simple geometric analysis based on the assumption of Bott (1959) and testing for rupture and friction laws; shear stress vs. normal stress (Angelier 1979, 1994). This paper summarizes knowledge concerning the direction and distribution of paleostress axes determined from fault-slip data, fold, tension gashes and relationships of mesostructures observed in the field. However, we are dealing neither with a detailed kinematic interpretation of the stress-induced deformation, nor with the magnitudes of the stress tensor parameters.

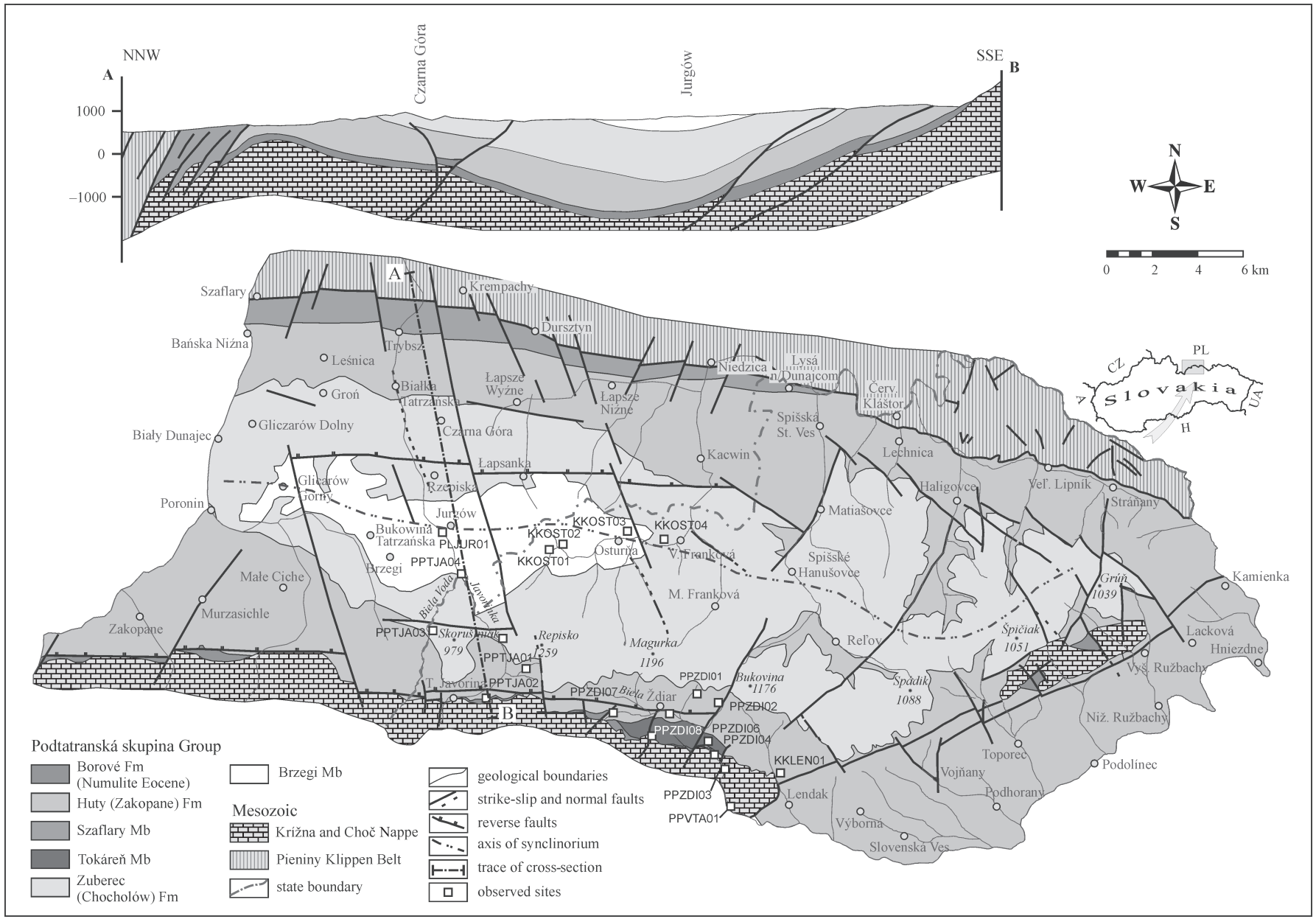

Fig. 1. Simplified tectonic map of the Spišská Magura Mts and the Podhale Synclinorium (according to Mastella 1975; Sliva 2005; Janočko et al. 2000a; Kępińska 1997; modified).

Geological setting

The Western Carpathians extend from the eastern end of the Eastern Alps toward the northeast, and are divided by the Pieniny Klippen Belt into the External and Central Western Carpathians (e.g. Andrusov 1958; Andrusov et al. 1973; Plašienka 1999). The investigated region has a complicated geological structure and, being located at this boundary zone, is affected predominantly by strong strike-slip deformation along this zone (Mastella 1975; Ratschbacher et al. 1993; Kováč & Hók 1996; Mastela et al. 1996; Marko et al. 2005).

The External Western Carpathians consist predominantly of Lower Cretaceous to Lower Miocene flysch formations deposited on an oceanic crust (e.g. Oszczypko 1992, 1998; Oszczypko-Clowes & Oszczypko 2005; Golonka et al. 2005 for the pre-Oligocene evolution) and/or a thinned continental crust (e.g. Winkler & Ślączka 1992; Jurewicz 2005). During the Late Oligocene to Middle Miocene subduction, the flysch formations were detached from their basement and thrust northward over the European Platform (Oszczypko & Ślączka 1989; Kováč et al. 1993; Plašienka et al. 1997; Kováč 2000).

The Pieniny Klippen Belt is a large-scale narrow shear zone forming the boundary which separates the accretionary wedge of the External Western Carpathians and the Central Western Carpathians. This zone includes the Kysuce, Czorsztyn, Orava and Klape successions, and is composed of Jurassic to Cretaceous rocks (Birkenmajer 1986; Jurewicz 2005; Plašienka & Jurewicz 2006; Plašienka et al. 2007). The deformation began during the Late Cretaceous (documented by synorogenic flysch formation), but the main brittle deformation in the Pieniny Klippen Belt occurred during the Paleogene to Neogene. The Eocene to Oligocene was characterized by dextral transpression which changed to Neogene dextral, later sinistral transpression and finally to sinistral transtensional tectonic regimes (Fodor 1995; Kováč 2000; Pešková et al. 2009).

The investigated territory of the Tatra Mts is located in the Central Western Carpathians which is composed of the Tatric and Fatric Units (e.g. Nemčok et al. 1993, 1994). The Tatric Unit is formed by the Variscan basement which consists of the Lower Paleozoic metamorphic sequences (para- and orthogneisses, mica schist and migmatite). These metamorphic sequences have been intruded by the Variscan granitoids. The basement is covered by an autochthonous sedimentary sequence with a stratigraphic range from Permian to mid-Cretaceous. The Tatric Unit is overthrust by the Fatric Unit (Krížna Nappe), which was derived from the area between the Tatric and Veporic realms (Biely & Fusán 1967). It consists mainly of the Triassic to middle Cretaceous sedimentary sequences (the Anisian Gutenstein Limestone and Carnian Carpathian Keuper are present in the study area). The age of the thrusting is documented by the deposition of synorogenic flysch (the Poruba Formation) during the Albian to Early Turonian in the Tatric cover sequences (Andrusov et al. 1973). The uppermost nappe structure is formed by the Hronic Unit (Choč Nappe) which is not present in the studied area. These nappes form a substratum of the Eocene to earliest Miocene sedimentation of the CCPB.

The Central Carpathian Paleogene Basin (Podtatranská skupina Group in the sense of Gross et al. 1984, 1993) is extended over approximately 9,000 km^2. Its sedimentary succession is predominantly composed of deep-marine siliciclastic sediments several hundred meters to several kilometers thick (Soták et al. 2001). The CCPB is interpreted as a forearc basin situated behind the Outer Carpathians accretionary wedge (Royden & Báldi 1988; Tari et al. 1993; Kázmér et al. 2003). The basement and the southern boundary of the CCPB is composed of the Central Carpathian units, and its northern boundary is the Pieniny Klippen Belt (Fig. 1), which represents a transpressional strike-slip zone related to a microplate boundary (Balla 1984; Csontos et al. 1992; Plašienka 1999). The inverted Paleogene basin of the Spišská Magura Mts is situated between the Tatra Mts and the Pieniny Klippen Belt. In the east, it is bounded by the Ružbachy fault and by the Mesozoic complexes of the Ružbachy Massif and in the west it gradually passes into the Podhale Basin (Figs. 1, 2). The Paleogene complex of the Spišská Magura Mts is a part of the CCPB and is formed by the Borové Formation, Huty Formation and Zuberec Formation (Marschalko & Radomski 1970; Gross et al. 1984; Janočko & Jacko 1999; Janočko et al. 2000a,b). The sedimentary deposits of the lower part of the Huty Formation in the Spišská Magura Mts are atypical and this formation can be considered to be coeval with the Šambron (Szaflary) Member developed in northern part of the Polish Podhale Basin (Watycha 1959; Westwalewicz & Mogilska 1986; Gedl 2000; Soták et al. 2001). This member can be related to global cooling and fall of the sea level (Janočko & Jacko 1999; Soták et al. 2001).

The hinge zone of the Podhale Synclinorium is composed of the Brzegi Member which is considered to be a distal facies of the Biely Potok Formation (Fig. 2; Watycha 1959; Gedl 2000; Sliva 2005). The sediments are Bartonian to Early Miocene in age (Olszewska & Wieczorek 1998; Gedl 2000).

Methods

Fault-slip and paleostress analysis

Faults and striae on the fault surfaces are very often present in rock masses and therefore kinematic and dynamic analysis of fault-slip data is a very popular tool for reconstruction of the paleostress fields. Standard procedures for brittle fault-slip analysis and paleostress reconstruction are now well established (Etchecopar et al. 1981; Michael 1984; Angelier 1990, 1994). In our work, the obtained data were registered into the NeotAct PostgreSQL database and were pre-processed using the LoCon software developed at the Department of Geology and Paleontology, Comenius University by Rastislav Vojtko. Later, these data were used in the Dieder and Shear modules using the TENSOR software package developed by Damien Delvaux (Delvaux 1993; Delvaux & Sperner 2003). The DIEDER program is an improved version of the Right Dihedron method of Angelier & Mechler (1977). It provides a determination of the four parameters of the reduced stress tensor and also allows a preliminary separation of the fault population into a homogeneous subset, broadly compatible with the computed stress tensor. Note that only complete fault-slip data, fault plane with slickenside lineation and known slip

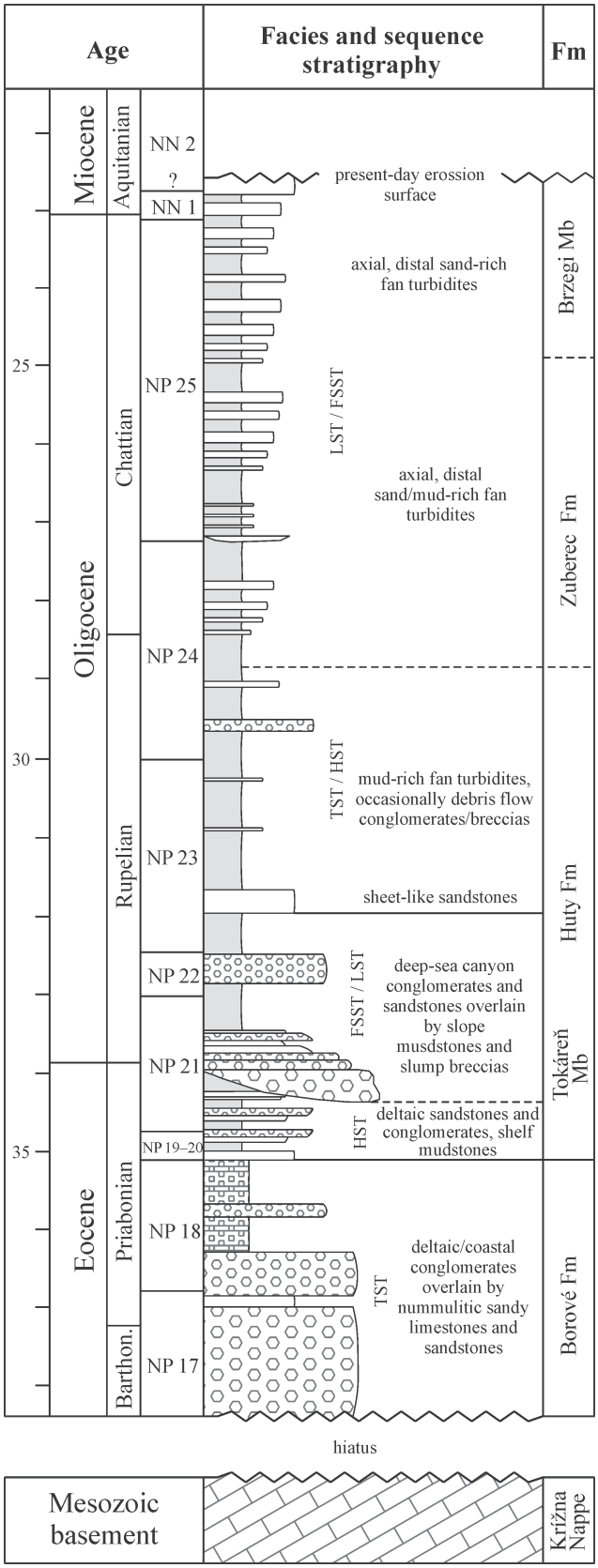

Fig. 2. Lithostratigraphical divisions of the Central Carpathian Paleogene Basin fill with respect to Slovak and Polish terminology (c.f. Soták 2001).

sense, are considered (for more details see Delvaux & Sperner 2003). The SHEAR program is an inversion method which is based on the assumption of Bott (1959) that slip on a plane occurs in the direction of the maximum resolved shear stress. Fault data were inverted to obtain the four parameters of the reduced stress tensor: σ_1 (maximum principal stress axis), σ_2 (intermediate principal stress axis) and σ_3 (least principal stress axis) and the ratio of principal stress differences is expressed by the formula:

$$\Phi = (\sigma_2-\sigma_3)/(\sigma_1-\sigma_3).$$

This parameter Φ defines the shape of the stress ellipsoid (Angelier 1989, 1994). The interpretation of results is also discussed for two important aspects: the quality assessment in view of the World Stress Map standards (Zoback 1992; Sperner et al. 2003) and the numerical expression of the stress regime as Stress Regime Index for regional comparisons and mapping (Delvaux & Sperner 2003). In accordance with the new ranking scheme for the World Stress Map project the quality ranges from A (best) to E (worst), and is determined as a function of threshold values of a series of criteria. The stress regime can be expressed numerically using an index Φ', ranking from 0.0 to 3.0 and defined as follows (see Delvaux et al. 1997):

- $\Phi' = \Phi$ where σ_1 is vertical (extensional stress regime);
- $\Phi' = 2 - \Phi$ where σ_2 is vertical (strike–slip stress regime);
- $\Phi' = 2 + \Phi$ where σ_3 is vertical (compressional stress regime).

Orientations of the stress axes (S_H — maximum horizontal compression axis, S_h — minimum horizontal compression axis, and S_v vertical axis), and the stress regime (Φ' between 0–1 for extensional regime, 1–2 for strike-slip regime, and 2–3 for compressional regime) are fully described by the average S_H azimuth (as defined in the World Stress Map by Müller et al. 2000) and the average stress regime index Φ' as defined above.

These methods (especially the inversion method) have some limitations which were the subject of criticism and its results were under discussion in specific situations (e.g. Dupin et al. 1993; Pollard et al. 1993; Nieto-Samaniego & Alaniz-Alvarez 1996; Twiss & Unruh 1998; Maerten 2000; Roberts & Ganas 2000). The basic point of stress computation by the inversion method is that regional stress tensor is spatially and temporally homogeneous in the whole-rock mass. These computations are influenced generally by the three effects which can occur in palaeostress analysis: 1) effect of ratio between the width and length of a fault; 2) effect of the Earth's surface (topoeffect); 3) effect of interaction between two or more faults (for further information see Pollard et al. 1993). These effects can misinterpret results of the paleostress analysis, but their influence is in most cases slight (Angelier 1994; Vojtko 2003).

Geometrical analysis of folds

The analysis of fold orientation was carried out using bedding planes, fold axes and planes measured during the field investigation. The principal deformational axes show the relationship to the fold geometry. The principal strain axis (A)

is parallel to the direction of the maximum elongation, the principal strain axis (C) is parallel to the shortening direction, and the principal strain axis (B) is parallel to the direction of the fold axis–axis of rotation (Ramsay 1967; Ramsay & Huber 1987; Marshak & Mitra 1988). The orientation of principal stress axes can be detected in terms of geometry of the folds. Fold axes are generally perpendicular to the maximum principal paleostress axis σ_1 (maximum compression). Fold axes and axial planes were constructed from measured fold limbs using the π pole method with the construction of β axes at the intersection of these limbs (Michael 1984; Marshak & Mitra 1988). Fold orientation, statistics and separation were computed and visualized with Fabric7 software application. The main principles of these methods are described in Wallbrecher (1986).

The fold structures were analysed in relation to the sedimentary fill and they were divided into (a) synsedimentary and (b) postsedimentary folds. The majority of folds appear to be related to reverse faulting and tilting which are often present and well-developed in the study area.

Tilting and chronology

During the field research, it was found that many fault-slips are affected by the tilting. The localities affected by tilting are located mainly at the foot of the Belianske Tatry Mts. The grade and direction of a rotation has been specified on the basis of bedding planes (S_0). For example, the bedding planes in the Blaščatská dolina Valley are S_0 14/33°. Based on this orientation, it is possible to extrapolate rotational axis

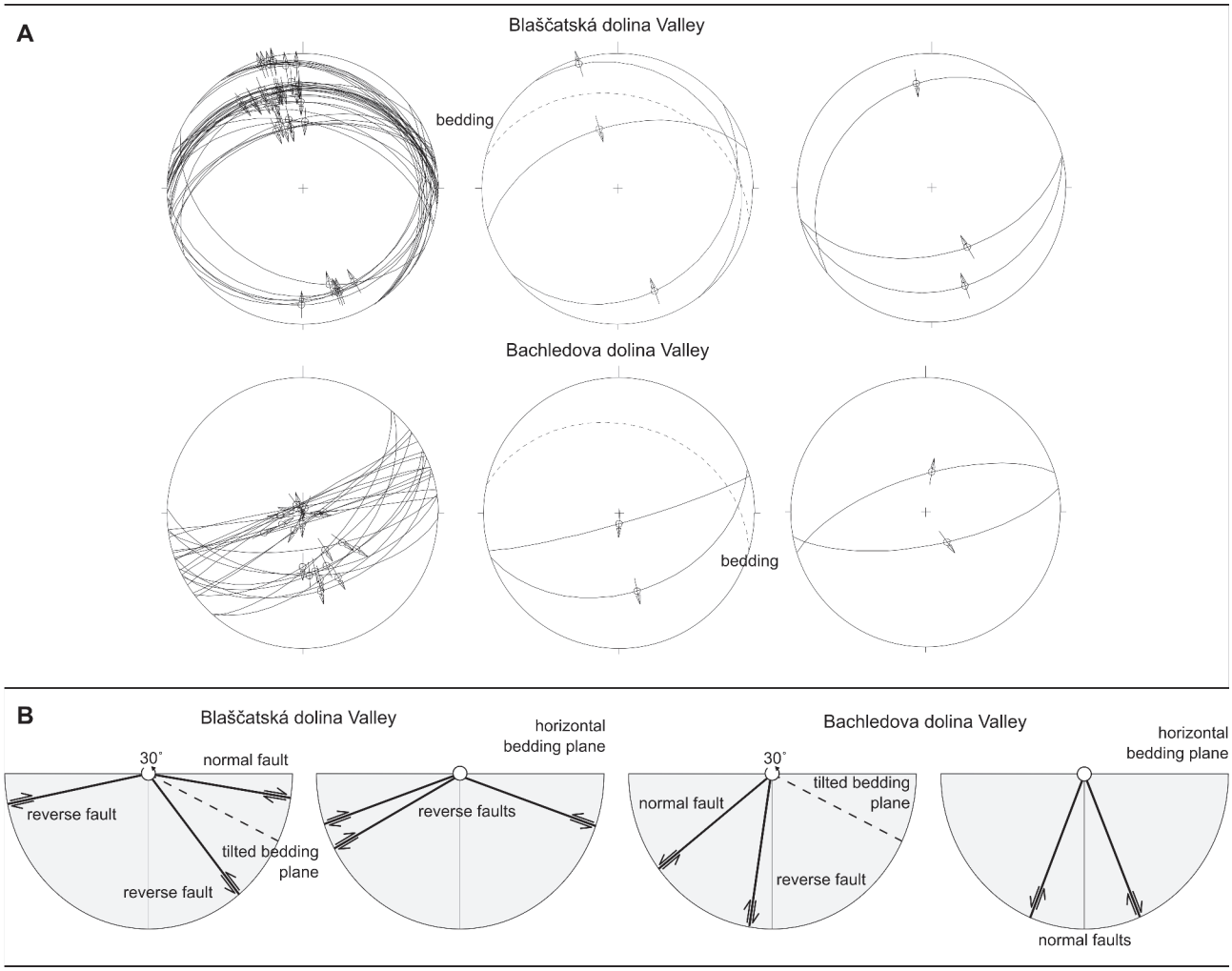

Fig. 3. Explanatory stereograms showing the tilting of the Tatra Mts. **A** — Orientation of the fault planes and slip lines with the sense of movement in stereograms. The left column shows the raw fault-slip data set; the middle column shows the schematic main fault systems in real position in the field (tilted faults; dip of bedding plane is approximately 30°); and the right column shows the schematic fault-slip data in the original position before tilting of bedding plane (faults are rotated into the position how they were developed). The fault-slip data are arranged into conjugate fault patterns. The stereograms were plotted in Lambert's projection in the lower hemisphere. **B** — Schematic faults with sense of movement. The first one shows the raw faults observed and measured in the field (tilted faults; dip of bedding plane is approximately 30°); and the right one shows the schematic faults in the original position before tilt rotation for both the Blaščatská and Bachledova dolina Valleys.

which has the value ρ 104/0° with rotational angle +33° using the equation:

ρ=dip direction (S_0) ± 90°.

A similar procedure was utilized for all sites disrupted by the tilting and allowed to separate fault structures into two groups on the basis of relation to tilting. Thus the rotated faults are older than the unrotated faults. The older faults have been divided into three homogeneous subsets and the younger faults also into three homogeneous subsets. After this procedure, it was possible to compute reduced paleostress tensors correctly (Fig. 3).

Data

Data obtained in the field from fault-slips, folds and extensional veins were used to reconstruct paleostress evolution in the study area. Data, collected in the Paleogene and Mesozoic sedimentary sequences, provide evidence that major deformational structures of the polyphase evolution resulted from reverse, strike-slip and normal faulting during the Neogene.

Meso-scale brittle failure structures used to study the state(s) of paleostress associated with faulting were measured at 14 sites. Fault orientation measurements and slip determinations made in the field, and results of geometrical and mathematical data analyses are presented in Fig. 4.

The fold data were measured mainly in the Eocene to Oligocene sedimentary sequences of the CCPB, less in the Krížna Nappe. The folds were used for determining the orientation of maximum shortening. Statistically, the mean trend of fold axes is 75/11° (calculated from both bedding attitudes and fold axes measurements), the data are quite robust and suggest the NNW-SSE shortening with maximal fluctuation of ±30° (Fig. 5a, Table 1). The fold axial planes are mainly inclined towards the north and they are considered to be generated by the "backthrust" tectonics with a general southern vergency during the Early and predominantly Middle Miocene (D_2 and D_4 stages). The fold set is almost pervasively developed along the northern boundary of the Tatra Mts and south of the Pieniny Klippen Belt. The folds are open to close with interlimb angles from 30° to 70°. The folds are often associated with the reverse faults (Fig. 6f).

Extension directions inferred from the total orientation pattern of extension vein walls and fibres show a preferred orientation of tension at the azimuth of 78° (Fig. 5b), less at the azimuth of 118°. We measured extensional veins at 16 localities and their orientations were also used to estimate deformational history and state of paleostress. Characteristically, the least principal axis determined from all veins (formed throughout the deformation history) is generally perpendicular to the most frequently observed NW-SE compresional axis of the transpressional tectonic regime. Development of the NNW-SSE vein system is older or partly synchronous with re-

Table 1: Orientation of principal fold axes. Explanations: **Site** — Code of locality; **n** — number of fold data used for determination of stress orientations; $\mathbf{n_T}$ — total number of fold data measured; **A** — axis of maximum elongation; **B** — intermediate axis (fold axis) and **C** — axis of maximum shortening.

Site	n	n_T	C	B	A
Tatranská Javorina — Javorinka valley (GPSinfo: N49°12'13", E019°32'57"), the Brzegy Beds					
PPTJA03A	2	2	172/27	076/11	326/61
Tatranská Javorina – Biela Voda (GPSinfo: E20°07'54"; N49°17'29"), the Brzegy Beds					
PPTJA04A	9	13	150/20	58/5	313/70
PPTJA04B	3	13	181/9	90/5	329/80
PPTJA04C	1	13	–	–	–
Ždiar — Biela creek (GPSinfo: E20°18'04"; N49°15'21"), the Huty Formation					
PPZDI06A	4	6	180/18	96/18	228/64
PPZDI06B	2	6	35/22	291/31	154/50
Lendak — Rieka stream (GPSinfo: E20°20'26"; N49°15'38"), the Huty Formation					
KKLEN01A	4	4	151/39	57/6	320/50
Osturňa IV. (GPSinfo: E20°15'54"; N49°20'22"), the Zuberec Formation					
KKOST04A	11	12	313/16	45/9	163/72
KKOST04B	1	12	182/0	272/17	95/73
Podspády — Príslop creak (GPSinfo: E20°11'33"; N49°17'02"), the Zuberec Formation					
PPTJA01A	8	9	343/16	77/12	201/70
PPTJA01B	1	9	51/0	141/17	325/73
Podspády – Nový creak (GPSinfo: E20°10'24"; N49°16'18"), the Borové Formation					
PPTJA02A	8	8	166/35	272/22	28/47
Ždiar — Bachledova valley (GPSinfo: E20°18'28"; N49°16'13"), the Huty Formation					
PPZDI02A	5	5	172/27	76/11	326/61
Ždiar — Tokáreň mount (GPSinfo: E20?16'02"; N49?15'38"), the Huty Formation					
PPZDI08A	1	1	59/0	149/7	329/83
Ždiar — Strednica (GPSinfo: E20?13'43"; N49?15'56"), the Huty Formation					
PPZDI07A	5	5	172/27	76/11	326/61
Jurgów — Bialka (GPSinfo:E20°07'15"; N45°22'45"), the Brzegy Beds					
PPJUR01A	2	5	114/16	272/73	22/6
PPJUR01B	3	5	335/1	65/8	237/82

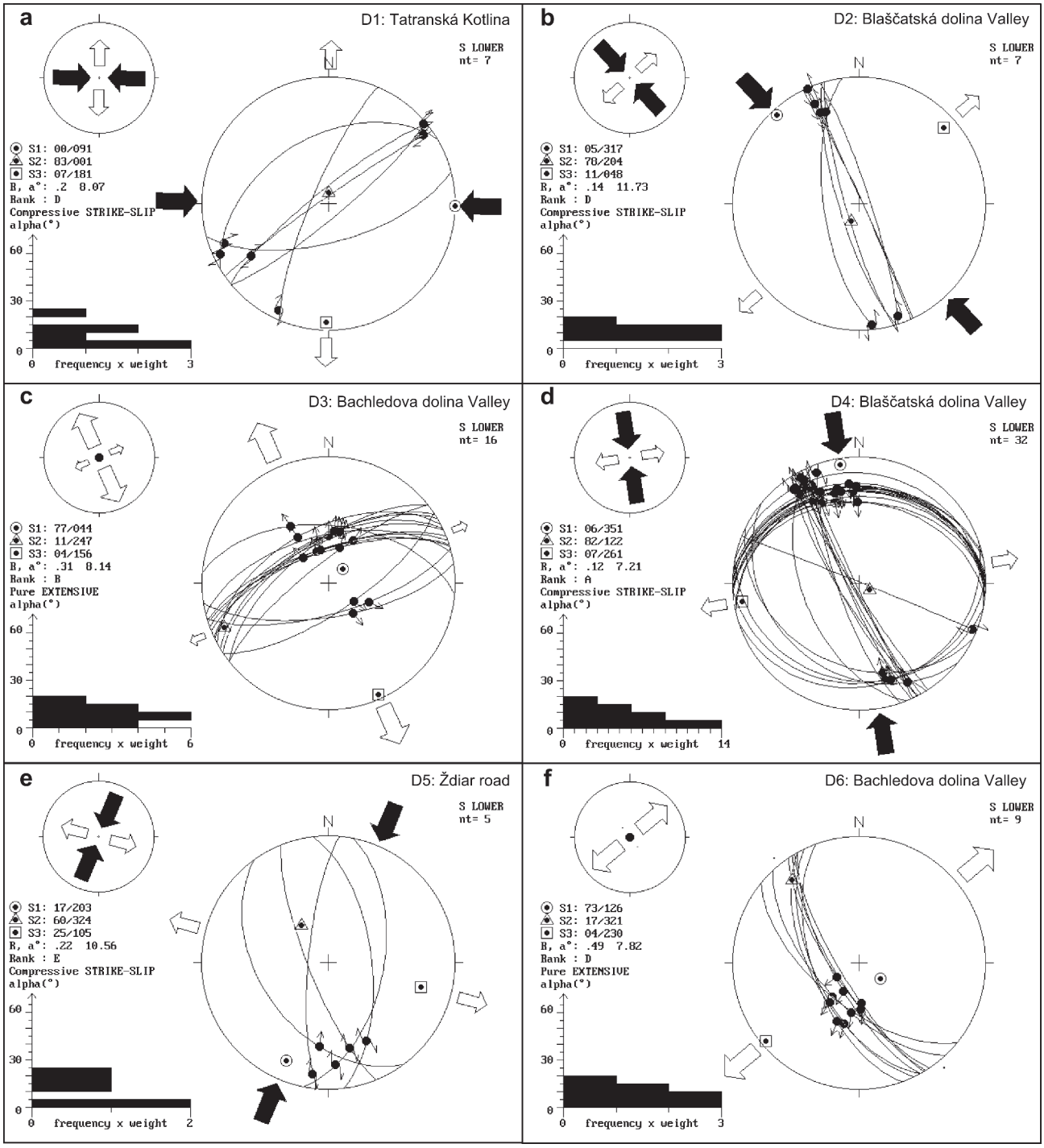

Fig. 4. Examples of paleostress reconstructions for the northern part of Spiš and the eastern part of Podhale regions. **a** — Late Eocene–Earliest Miocene phase recorded at the Tatranská Kotlina locality (site code PPVTA01A); S_0 — 55/35°. **b** — Early Miocene phase; the Ždiar — Blaščatská dolina locality (site code PPZDI01A); S_0 — 14/33°. **c** — Early/Middle Miocene phase; the Ždiar — Bachledova dolina locality (site code PPZDI02A); S_0 — 16/30°. **d** — Middle Miocene (Late Badenian) phase; Ždiar — Blaščatská dolina locality (site code PPZDI01D); S_0 — 14/33°. **e** — Late Miocene phase; the Ždiar — road locality (site code PPZDI03F); S_0 — 1/27°. **f** — Early/Middle Miocene phase; the Ždiar — Bachledova dolina locality (site code PPZDI02F). Explanation: Stereogram (Lambert's net, lower hemisphere) with traces of fault planes, observed slip lines and slip senses, histogram of observed slip-theoretical shear deviations for each fault plane and stress map symbols. $\mathbf{S_1}=\boldsymbol{\sigma_1}$, $\mathbf{S_2}=\boldsymbol{\sigma_2}$ and $\mathbf{S_3}=\boldsymbol{\sigma_3}$ — azimuth and plunge of principal stress axes; $\mathbf{R}=\boldsymbol{\Phi}$ — stress ratio ($\boldsymbol{\sigma_2}$–$\boldsymbol{\sigma_3}$/$\boldsymbol{\sigma_1}$–$\boldsymbol{\sigma_3}$); $\boldsymbol{\alpha}$ — mean slip deviation (in °); **Rank** — quality ranking scheme according to World Stress Map project from A (best) to E (worst) as a function of several criteria (c.f. Sperner et al. 2003), and $\mathbf{S_0}$ — bedding planes.

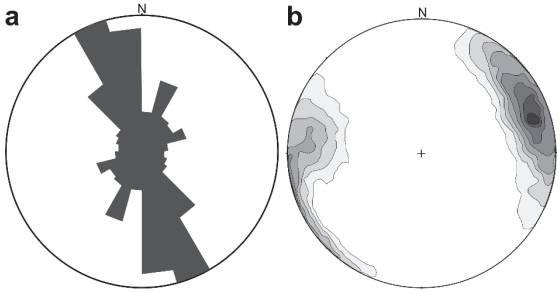

Fig. 5. Contour plot of all measured and constructed fold axes and Rose diagram of extensional veins. **a** — Contour plot of fold axes. Report counting: number of data points 98, number of points in maximum 30 (=30.61%), number of contours 8, distance between contours 3.75 (=3.83 %). Contours shown data points in %: 3.75 pts=3.83 %, 7.50 pts=7.65 %, 11.25 pts=11.48 %, 15.00 pts=15.31 %, 18.75 pts=19.13 %, 22.50 pts=22.96 %, 26.25 pts=6.79 %, 30.00 pts=30.61 %. Lambert projection, lower hemisphere. **b** — Rose diagram of extensional veins. Report rose: total data 204, class interval 15°, symmetrical (0–180°) non-weighted data, and maximum 20.10 %.

spect to tilting, whereas the second NNE-SSW vein system is synchronous with, or postdates tilting.

Review of the Cenozoic stresses and chronology of faulting

The evolution of the orogen, the age of the principal deformational events, basin evolution and destruction, and also the relative chronology of these structures are also important preconditions of successful paleostress analysis. The separated phases in the study area were also compared to regions which have similar Oligocene to Quaternary evolution (Kováč & Hók 1996; Fodor et al. 1999; Jacko & Janočko 2000; Pešková et al. 2009).

Tectonic regime before and during the sedimentation of the CCPB sedimentary sequence (Late Cretaceous to Oligocene)

The oldest recorded deformational phase (D_1) is characterized by the E–W compression and N–S extension (Paleocene–pre-Middle Eocene). This strike-slip tectonic regime was determined predominantly in the Mesozoic rocks of the Krížna Nappe (Figs. 4a, 7) where it is very common. Compressive stresses were resolved mainly by movements along WNW-ESE trending sinistral and WSW-ENE trending dextral shears. These faults are pre- and synsedimentary with respect to the CCPB, because of the similar orientation of paleostress field was seldom observed in sites located in the CCPB (Fig. 7), where the principal compressional axis (σ_1) is slightly rotated (about 30°) into the WNW-ESE position.

Tectonic regimes after sedimentation of the CCPB sedimentary sequence and before tilting of the Tatra Massif (Eggenburgian to Badenian)

After deposition of the CCPB sequences, the new strike-slip to compressive deformational phase (D_2) characterized by NW-SE compression and NE-SW tension started in the Eggenburgian (Table 2). This is the oldest tectonic regime which was well identified in the Oligocene sediments (Fig. 7). The principal maximum (σ_1) and the least (σ_3) principal stress axes were subhorizontal, while the principal intermediate axis (σ_2) was in subvertical position. This phase is predominantly characterized by N-S oriented sinistral strike-slip and W-E oriented dextral strike-slip faults, sporadically with NE-SW trending reverse faults. Nice examples of this deformation are Zakopane — Biały Creek, Ždiar — Blaščatská dolina Valley, Tatranská Javorina — Javorinka and Jurgów localities.

The extensional tectonic regime (D_3) occurred at the end of this deformational phase and can be divided into two subphases. The older one is dominantly NE-SW oriented tension (D_{3a}) and the second one is generally oriented in a NNW-SSE direction (D_{3b}). Note that the evaluation of the subphase chronology was solved using successive fault slips where the older fault population is offset by younger faults. The NE-SW tension is poorly preserved and is considered to be the final stage of the NW–SE compression (Fig. 7). The tension is characterized predominantly by neoformed normal and less by inherited oblique-normal faults (Fig. 6c).

Tectonic regimes during and after tilting of the Tatra Massif (Sarmatian to Quaternary)

During the tilting of the Tatra Massif a new compressional to transpressional tectonic regime (D_4) occurred. Evolution of this tectonic regime is complex, but generally consists of two subphases which were tenuously dated at Sarmatian to Pannonian.

The first subphase (D_{4a}) is mainly characterized by the compressional tectonic regime with orientation of the principal maximum stress axis in the NNW-SSE direction. The stress relaxed on the newly formed E-W conjugate reverse or NW-SE dextral strike-slip faults (Fig. 4d). Fault structures activated during this subphase were observed at many places in the study area (Fig. 7, Table 2) and are accompanied by remarkable folds (Fig. 5a). This deformation event occurred just before the tilting of the Tatra Massif. The conspicuous reverse faulting with SSE vergence dominates this deformational stage (Fig. 6a,b,d) which is connected with back-thrusting in the northern part of the Central Western Carpathians (e.g Plašienka et al. 1998; Marko et al. 2005; Pešková et al. 2009). Deformation is also characterized by widespread folding under semi-brittle to brittle conditions. Generally, the folds are open to close.

The predominantly compressional tectonic regime was continuously followed by a pure transpressional tectonic regime of the second subphase (D_{4b}) which occurred during the final stage of the Tatra Massif tilting. During this N-S compression and perpendicular tension, the NNW–SEE dextral and NNE–SSW sinistral strike slip faults were activated as newly formed or inherited on weakness planes. This deformation is very conspicuous at many localities (Fig. 7, Table 2).

The preceding deformational phase (D_{4b}) most likely passed continuously into a transtensional tectonic regime

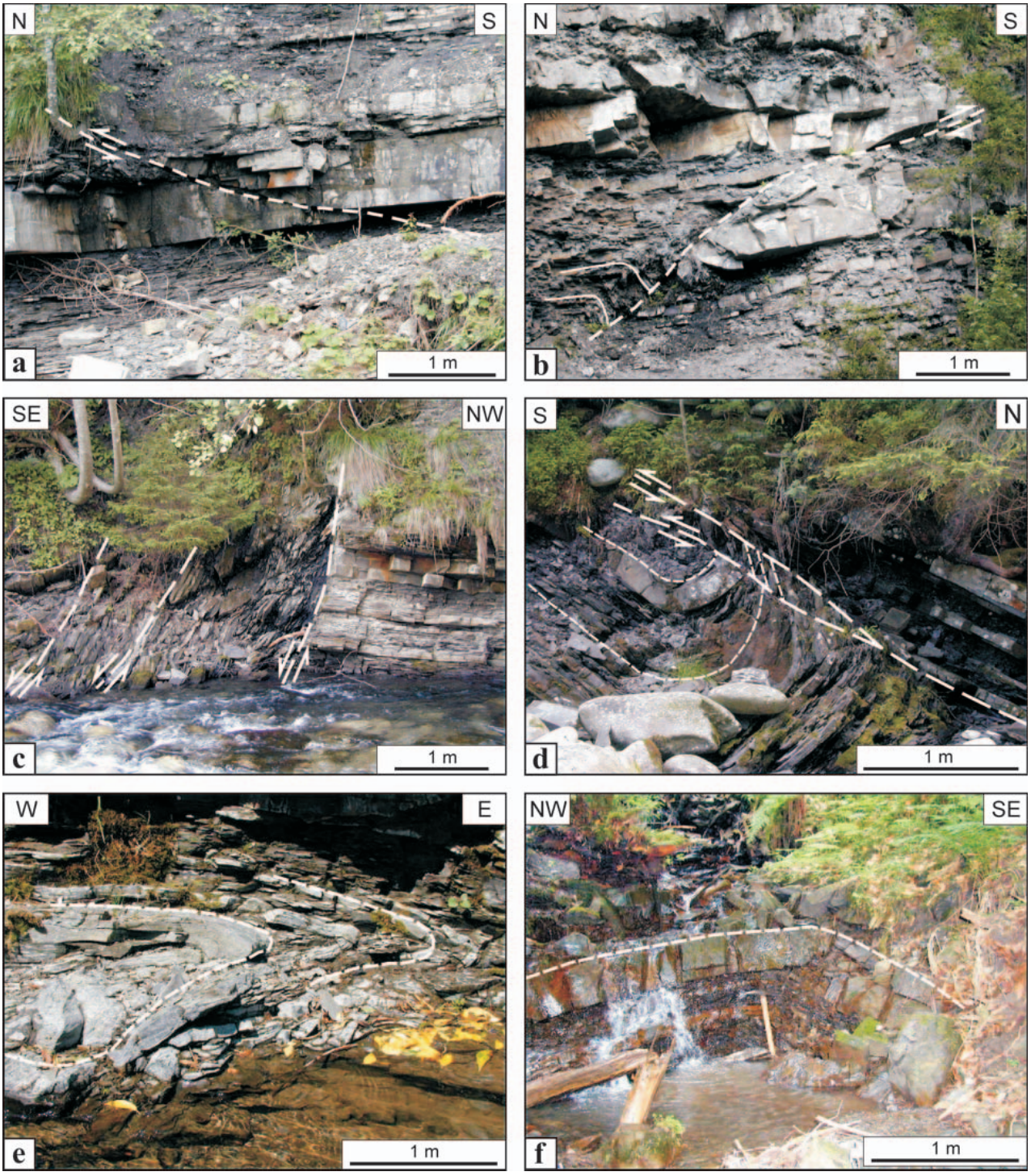

Fig. 6. Field photos of mesostructures. **a** — small scale reverse fault of the D4a stage (Tatranská Javorina site PPTJA03). **b** — small scale reverse fault associated with drag fold of the D4a stage with south-verging (Tatranská Javorina site PPTJA03). **c** — large scale normal fault, the fault zone is approximately 4 m thick (Tatranská Javorina site PPTJA01). **d** — large scale reverse fault associated with well-developed drag folds in the footwall (Tatranská Javorina site PPTJA03). **e** — tight slump fold (Osturňa site KKOST04). **f** — hinge area of slightly asymmetric, south-verging macroscopic fold (Tatranská Javorina site PPTJA01).

with orientation of the principal maximum stress axis in NE–SW direction (D_5). During this tectonic regime, generally the N-S dextral strike-slip faults and ENE-WSW sinistral strike-slip faulting were generated. Some of them were inherited weakness planes of previous deformational phases.

Neotectonics

The youngest stage D_6 (?Pontian–Quaternary) is characterized by a weak extensional tectonic regime which can be divided into two subphases. The first one is NW–SE (D_{6a}) and

Fig. 7. Chronology of deformational phases at single sites. In the lower part of the table are sites arranged from the oldest rock sequence on the left side (Tatranská Kotlina) to the youngest rock sequence on the right side (Jurgów). Dark grey represents the Triassic formation of the Krížna Nappe and light grey the Late Eocene to Oligocene formations of CCPB (see Table 2). On the left side of the table are the main geological phases which occurred in the investigated area with indices.

Table 2: Paleostress tensors from fault slip data. Explanations: **Site** — Code of locality; **n** — number of fault used for stress tensor determination; $\mathbf{n_T}$ — total number of fault data measured; $\mathbf{S1=\sigma_1}$, $\mathbf{S_2=\sigma_2}$ and $\mathbf{S_3=\sigma_3}$ — azimuth and plunge of principal stress axes; $\mathbf{R=\Phi}$ — stress ratio (S_2–S_3/S_1–S_3); **α**—mean slip deviation (in °); **Q** — quality ranking scheme according to the World Stress Map Project (Sperner et al. 2003); **R'** — tensor type index as defined in the text (for further information see Delvaux et al. 1997).

Site	n	n_T	σ_1	σ_2	σ_3	Φ	α	Q	Φ'
Žďiar — Blaščatská dolina quarry (GPSinfo: E20°17'13"; N49°16'11"), the Huty Formation									
PPZDI01A	7	107	317/5	204/78	48/11	0.14	11.73	D	1.86
PPZDI01B	13	107	106/85	262/4	352/3	0.36	4.19	C	0.36
PPZDI01C	4	107	98/74	226/9	318/12	0.51	3.47	E	0.51
PPZDI01D	18	107	172/4	81/6	298/82	0.39	7.44	B	2.39
PPZDI01E	32	107	351/6	122/82	261/7	0.12	7.21	A	1.88
PPZDI01F	8	107	332/0	62/16	241/7	0.25	7.78	D	2.25
PPZDI01G	8	107	190/78	62/7	331/9	0.38	2.54	D	0.38
PPZDI01H	7	107	126/83	2340/6	250/4	0.41	8.19	D	0.41
Žďiar — Bachledova dolina quarry (GPSinfo: E20°18'28"; N49°16'13"), the Huty Formation									
PPZDI02A	16	58	44/77	247/11	156/4	0.31	8.14	B	0.31
PPZDI02B	7	58	278/74	145/11	53/11	0.58	11.59	D	0.58
PPZDI02C	3	58	61/74	314/5	222/16	–	–	E	–
PPZDI02D	1	58	257/25	153/27	9/58	–	–	E	–
PPZDI02E	12	58	351/70	253/3	162/20	0.52	6.03	C	0.52
PPZDI02F	9	58	126/73	321/17	230/4	0.49	7.82	D	0.49
Tatranská Javorina — Biela Voda (GPSinfo: E20°07'54"; N49°17'29"), the Zuberec Formation									
PPTJA04A	5	38	216/82	44/7	314/1	0.43	6.94	E	0.43
PPTJA04B	12	38	335/10	66/7	191/78	0.40	10.17	C	2.40
PPTJA04C	7	38	166/2	76/2	218/88	0.72	5.30	D	2.72
PPTJA04D	8	38	195/77	22/13	292/2	0.21	4.31	D	0.21
Podspády — Nový creek (GPSinfo: E20°10'24"; N49°16'18"), the Huty Formation									
PPTJA02A	2	3	109/38	206/8	306/51	–	–	E	–
PPTJA02B	1	3	160/52	206/8	356/37	–	–	E	–
Podspády — Príslopský creek (GPSinfo: E20°11'33"; N49°17'02"), the Zuberec Formation									
PPTJA01A	1	2	105/70	272/20	3/4	–	–	E	–
PPTJA01B	1	2	4/16	273/2	176/74	–	–	E	–
Tatranská Kotlina — quarry (GPSinfo: E20°18'49"; N49°13'53"), the Gutenstein Limestone									
PPVTA01A	7	15	91/0	1/83	181/7	0.20	8.07	D	1.8
PPVTA01B	2	15	140/7	231/10	15/78	–	–	E	–
KKLEN01A	5	5	169/76	47/7	316/12	0.74	6.60	E	0.74
Žďiar — road (GPSinfo: E20°16'30"; N49°16'13"), the Carpathian Keuper Formation									
PPZDI03A	7	37	284/38	107/52	15/1	0.62	16.01	E	1.38
PPZDI03B	4	37	246/74	118/10	26/13	0.41	4.70	E	0.41
PPZDI03C	12	37	265/88	21/1	111/2	0.37	12.8	D	0.37
PPZDI03D	5	37	181/20	294/47	76/36	0.36	4.68	E	0.36
PPZDI03E	4	37	1/22	96/12	212/65	0.35	8.47	E	2.35
PPZDI03F	5	37	203/17	324/60	105/25	0.22	10.56	E	1.78
Žďiar — Biela (GPSinfo: E20°18'09"; N49°15'12"), the Carpathian Keuper Formation									
PPZDI04A	5	16	329/11	236/13	98/73	0.47	15.82	E	2.47
PPZDI04B	11	16	31/85	206/5	296/0	0.50	9.57	C	0.5
Žďiar — Biela (GPSinfo: E20°18'04"; N49°15'21"), the Borové & Huty Formations									
PPZDI06A	14	14	150/6	241/11	29/77	0.47	5.20	C	2.47
Žďiar — Tokáreň (GPSinfo: E20°16'02"; N49°15'38"), the Tokáreň Beds									
PPZDI08A	9	12	168/23	19/64	263/12	0.51	6.99	D	1.49
PPZDI08B	3	12	160/78	349/12	259/2	–	–	E	–
Jurgów (GPSinfo: E20°16'02"; N49°15'38"), the Brzegy Beds									
PLJUR01A	3	6	114/16	272/73	22/6	–	–	E	–
PLJUR01B	3	6	335/1	65/8	237/82	–	–	E	–

the second one is ENE–SWS oriented tension (D_{6b}) which is considered to be younger than the previous one. However, there are no direct data to prove this assumption. A Pliocene to Quaternary extensional tectonic regime was also observed in the northern part of the Orava region (Pešková et al. 2009). These deformation subphases have been recorded at many localities (Fig. 7) and their reduced stress tensors are described in Table 2.

Discussion

Fault-slip analysis and paleostress reconstruction

The tectonic structures measured in the study area reveal changes of paleostress fields during the Cenozoic Era. These changes were caused by rotation of the paleostress field, by spin rotation of crustal blocks (Márton et al. 1999) and by

tilting of the Tatra Massif. It means that older deformational phases are affected by these rotations. Based on this assumption, it is possible to determine chronology of faulting in the study area.

An important result of the paleostress reconstruction was the E-W orientation of σ_1 and perpendicular σ_3 axes of the strike-slip tectonic regime (D_1) which has only been measured in the Mesozoic rocks of the Fatric Unit and is considered to be of Paleocene–Eocene age, because it is practically absent in the Oligocene to lowest Miocene strata. This is in accordance with the results of data measured in the Orava region (Pešková et al. 2009), in the Slovenské rudohorie Mts (Vojtko 2003) and also in the hinterland (southern part) of the Western Carpathians and Pannonian Basin (e.g. Fodor et al. 1992, 1999; Budai et al. 2008). We assume that it is a former N-S compression event which was recorded and fixed in the host rocks before the Early and Middle Miocene counter-clockwise spin rotation of crustal blocks.

The tilting of the Tatra Massif had a crucial implication for the kinematic interpretation and subsequently for the timing of the paleostress stages. The tilting was most likely the result of the NNW–SSE to N–S oriented compression. The effect of tilting caused (1) the rotation of the original conjugated reverse faults into the normal faults with unordinary very low (<5°) north dipping planes with identical types of striae (mineral accretionary steps and slickenfibers); (2) the original normal faults rotated into position of the steeply (more than 75°) north dipping reverse faults (Fig. 3). The faulting was observed predominantly in the Blaščatská and Bachledova dolina Valleys and in the bedrock of the Biela River near the village of Ždiar. The youngest tectonic regime with the horizontal NE-SW trending σ_1 is Late Neogene in age.

Tectonic evolution during the Cenozoic Era

The Paleogene to Middle Eocene tectonic processes were controlled by approximately W-E oriented compression under compressional to transpressional tectonic regimes. Predominantly during the Eocene to Oligocene, the studied area was located on a convergent plate margin along the CWC edge. The flysch sedimentation occurred not only on the lower plate (the Magura Basin), but also on the frontal part of the overriding continental plate (CCPB). The flexure of this overriding continental plate was most likely generated by subcrustal erosion of lower crustal elements of the overriding plate that had been accreted to the upper plate during the preceding subduction period (Wagreich 1995; Kázmér et al. 2003), and/or extensional collapse of the overthickened rear of the External Carpathian thrust wedge (Súľov phase — Plašienka 2002; Plašienka & Jurewicz 2006). The CCPB was formed as a marginal basin of the Paratethys. It shows a fore-arc position extended on the destructive plate margin and behind the Outer Carpathian accretionary wedge (Soták & Starek 2000; Soták et al. 2001). The final collision of the Western Carpathian orogenic wedge with the North European Platform resulted in the closure and destruction of the Paleogene fore-arc basin above the active CWC thrust front during the Early Miocene (Kováč 2000). Based on the orientation of the compression of the D_1 phases (oblique to the Pieniny Klippen Belt), we assume that subduction of the oceanic crust was oblique to the ALCAPA (Alpine-Carpathian-Pannonian) microplate edge. Inversion of the CCPB, connected with the D_2 deformational phase, is dated to the Early Miocene (?Ottnangian), because the youngest known sediments are Egerian–Eggenburgian in age (Soták et al. 2001). The youngest known sediments of the Magura Nappe in the External Western Carpathians have the same age (e.g. Oszczypko et al. 2005). Unlike Sperner (1996) and Sperner et al. (2002), we suppose that the D_{1-3} tectonic regimes only weakly influenced the uplift of the Tatra Mountains. Compressive structures (approximately E-W trending fold axes) are also developed in the Šambron-Kamenica Zone which is connected with the Early Miocene compressional tectonic regime (Plašienka et al. 1998). However, the results of our paleostress analysis point out that the compressional tectonic regime (D_{4-5}) with the general N-S compression is most probably younger, Middle Miocene in age.

Maximum intensity of uplift and tilting of the Tatra Mountains is dated as Middle/Late Miocene based on fission-track data from apatites (10–19 Ma — Kováč et al. 1994; 15 Ma — Kráľ 1977; Baumgart-Kotarba & Kráľ 2002). The amount of the Neogene uplift of the Tatra region is not precisely known.

The neotectonics of the Tatra Mountains area (D_6) is very interesting for the very high amplitude of mountain uplift and remarkable features of their relief. Neotectonic evolution of the area occurred along weakness planes, inherited faults and neoformed fault structures. The Tatra Mountains were uplifted and the area of the Podhale Synclinorium relatively subsided. The uplift can be considered to be quite intensive and differentiated and the relative uplift is estimated at about 350–450 m according to correlation of Lower Pleistocene horizons (see Nemčok et al. 1993).

Pliocene to Quaternary uplift of the Tatra Massif, especially in the north-western part, was studied by Bac-Moszaszwili (1993). Very young normal faulting along the W-E trending faults was also observed at the Vikartovce fault (Marko et al. 2008; Vojtko et al. 2009) which can be correlated with the Subtatra fault system. Active tectonics and movements along the faults during the neotectonics phase in the Tatra Mts and related areas has also been documented by many other authors using various methods (e.g. Zuchiewicz 1995, 1998; Baumgart-Kotarba 1981; Birkenmayer 1986; Baumgart-Kotarba & Ślusarczyk 2001).

Relation to the Pieniny Klippen Belt

During the Early Miocene, the Pieniny Klippen Belt (PKB) zone was under dextral transpression with the development of positive flower structures (e.g. Ratschbacher et al. 1993; Marko et al. 2005; Plašienka & Jurewicz 2006; Pešková et al. 2009). The internal boundary of the PKB was affected by reverse faulting and folding (Mastella 1975; Mastella et al. 1996; Kępińska 1997; Plašienka et al. 1998). Generally, the PKB is a subvertical narrow zone in which strike-slipping prevailed and led to the formation of the typical block-in-matrix tectonic style caused by pervasive brittle faulting (Birkenmayer 1996; Plašienka & Jurewicz 2006). Complex, compressional through transpressional to transtensional tectonic regimes along the PKB dominated during the Middle to Late Neogene.

Stresses were also relaxed by dextral strike-slips and oblique-slips along synthetic shears parallel to the WNW-ESE trending PKB. During the Late Neogene to Quaternary, the sinistral transtension along the PKB was followed by a general tension which segmented the zone by dextral and normal NNE–SSW to N–S faults (Fig. 1).

Conclusion

The reconstruction of the paleostress field was carried out using the fault-slip, fold and vein data in the Spišská Magura and Tatra region. The computer analyses of structural measurements, as well as field geological and structural studies show a generally clockwise rotation of the paleostress field during the Neogene. One principal phase was distinguished as being Paleocene to Oligocene, four phases as Miocene and the last one as Pliocene to Quaternary in age (Fig. 7).

The E–W oriented compression and N–S tension are recorded in the Triassic sequences of the Fatric Unit and are very poorly preserved in the sedimentary sequences of the CCPB. This oldest tectonic phase (D_1) is dated to the Paleocene–Oligocene and indicates a pure strike-slip tectonic regime.

Post-sedimentary deformation of the CCPB (Early Miocene) was characterized by a compressional to transpressional tectonic regime (D_2) which successively changed to an extensional tectonic regime (D_3) at the boundary between the Early and Middle Miocene (more or less Karpatian to Early Badenian stages).

The poorly preserved extensional tectonic regime of D_3 tectonic phase finished most probably in the Badenian stage and was replaced by a new compressional tectonic regime (D_4) with the NNW–SSE trending principal maximum stress axis (σ_1). The paleostress field rotated progressively clockwise from the NNW–SSE to the N–S position and the Tatra Massif was simultaneously tilted. This tectonic phase can be divided into two subphases based on the relationship between the faults and tilt rotation of the Tatra Massif. The older one (D_{4a}) is a predominantly compressional less transpressional phase with the orientation of the principal maximum paleostress axis in the NNW-SSE direction. The structures of this subphase are affected by tilting. The orientation of the σ_1 of the second subphase (D_{4b}) is approximately in the N–S and the measured structures are more or less in the autochthonous position. During this tectonic regime, intensive backthrusting which propagated toward the south occurred. The last transpressive tectonic regime (NE–SW oriented σ_1) was tenuously dated to the Pannonian stage (D_5).

The youngest tectonic regime (D_6) is characterized by an extensional tectonics which can be divided into two subphases. The first one (D_{6a}) is NW–SE and the second one is ENE–SWS oriented tension (D_{6b}) and is considered to be younger than the previous one based on the cross-cutting relationship of the observed faults.

Acknowledgments: This paper is based on the main part of the diploma thesis undertaken during the years 2003–2005 by Eva Tokárová who passed away in 2007. We dedicate this article to her memory. Our work was supported by the Slovak Research and Development Agency under contracts Nos. APVV-0158-06 and APVV-0465-06. The authors wish to thank Damien Delvaux for the TENSOR, Eckart Wallbrecher & Wolfgang Unzog for the Fabric7 software applications and we are indebted to László Fodor and an anonymous reviewer for careful reviewing and suggestions to improve the paper.

References

Andrusov D. 1958: Geology of Czechoslovak Carpathians. Part 1. *SAV Publisher*, Bratislava, 1–304 (in Slovak).

Andrusov D., Bystrický J. & Fusán O. 1973: Outline of the structure of the West Carpathians. Guide book, X. Congress CBGA. *GÚDŠ*, Bratislava, 44.

Angelier J. 1979: Determination of the mean principal directions of stress for a given fault population. *Tectonophysics* 56, T17–T26.

Angelier J. 1989: From orientation to magnitudes in paleostress determinations using fault slip data. *J. Struct. Geol.* 11, 1, 2, 37–50.

Angelier J. 1990: Inversion of field data in fault tectonics to obtain the regional stress — III. A new rapid direct inversion method by analytical means. *Geophys. J. Int.* 103, 363–376.

Angelier J. 1994: Fault slip analysis and paleostress reconstruction. In: Hancock P.L. (Ed.): Continental deformation. *Pergamon Press*, University of Bristol (U.K.), London, 53–100.

Angelier J. & Mechler P. 1977: Sur une méthode graphigue de recherche des contraintes principles également utilisable en tectonique et en séismologie: la méthode des dièdres droits. *Bull. Soc. Géol. France* 19, 1309–1318.

Bac-Moszaszwili M. 1993: Structure of the western termination of the Tatra massif. *Ann. Soc. Geol. Pol.* 63, 167–193.

Balla Z. 1984: The Carpathian loop and the Pannonian basin. A kinematic analysis. *Geophys. Trans.* 30, 313–353.

Baumgart-Kotarba M. 1981: Tectonic movement on the eastern Podhale in the light of an analysis of Quaternary terraces of the Białka Tatrzańska valley and the lineaments from satellite image. *Przegl. Geogr.* 53, 725–736 (in Polish, English summary).

Baumgart-Kotarba M. & Kráľ J. 2002: Young tectonic uplift of the Tatra Mts. (Fission track data and geomorphological arguments). Proceedings of XVII. Congress of Carpathian-Balkan Geological Association. *Geol. Carpathica*, *Spec. Issue* 53 (CD version).

Baumgart-Kotarba M., Dec J. & Ślusarczyk R. 2001: Quaternary tectonic grabens of Wróblówka and Pieniążkowice and their relation to Neogene strata of the Orava Basin and Pliocene sediments of the Domański Wierch series in Podhale, Polish West Carpathians. *Stud. Geomorph. Carpatho-Balcanica* 35, 101–119.

Biely A. & Fusán O. 1967: Zum Problem der Wurzelzonen der subtatrischen Decken. *Geol. Práce, Spr.* 42, 51–64.

Birkenmayer K. 1986: Stages of structural evolution of the Pieniny Klippen Belt. Carpathians. *Stud. Geol. Pol.* 88, 7–32.

Bott M.H.P. 1959: The mechanics of oblique slip faulting. *Geol. Mag.* 96, 109–117.

Budai T., Császár G., Csillag G., Fodor L., Gál N., Kercsmár Zs., Kordos L., Pálfalvi S. & Selmeczi I. 2008: Geology of the Vértes Hills. Regional map series of Hungary. (Explanatory Book to the Geological Map of the Vértes Hills 1:50,000). *MAFI*, Budapest, 1–368.

Csontos L., Nagymarosy A., Horváth F. & Kováč M. 1992: Tertiary evolution of the Intra-Carpathian area: a model. *Tectonophysics* 208, 221–241.

Delvaux D.F. 1993: The TENSOR program for palaeostress reconstruction: examples from the east African and the Baikal rift zones. *Terra Nova, 5, suppl. 1, Proceedings of EUG VII, Strasbourg, 4–8 April.*, 1–216.

Delvaux D. & Sperner B. 2003: New aspects of tectonic stress inver-

sion with reference to the TENSOR program. In: Nieuwland D.A. (Ed.): New insights into structural interpretation and modelling. *Geol. Soc. London, Spec. Publ.* 212, 75–100.

Delvaux D., Moyes R., Stapel G., Petit C., Levi K., Miroshnichenko A., Ruzhich V. & Sankov V. 1997: Paleostress reconstructions and geodynamics of the Baikal region, Central Asia. Part 2. Cenozoic rifting. *Tectonophysics* 282, 1–38.

Dupin J.M., Sassi W. & Angelier J. 1993: Homogeneous stress hypothesis and actual fault slip: a distinct element analysis. *J. Struct. Geol.* 15, 8, 1033–1043.

Etchecopar A., Vasseur G. & Daignieres M. 1981: An inverse problem in microtectonics for the determination of stress tensor from fault striation analysis. *J. Struct. Geol.* 3, 51–65.

Fodor L. 1995: From transpression to transtension: Oligocene–Miocene structural evolution of the Vienna Basin and the East Alpine–Western Carpathian junction. *Tectonophysics* 242, 151–182.

Fodor L., Magyari A., Kázmer M. & Fogarasi A. 1992: Gravity-flow dominated sedimentation on the Buda paleoslope (Hungary): Record of Late Eocene continental escape of the Bakony unit. *Geol. Rdsch.* 695–716.

Fodor L., Csontos L., Bada G., Györfi I. & Benkovics L. 1999: Tertiary tectonic evolution of the Pannonian Basin system and neighbouring orogens: a new synthesis of palaeostress data. In: Durand B., Jolivet L., Horváth F. & Séranne M. (Eds.): The Mediterranean Basins: Tertiary extension within the Alpine Orogen. *Geol. Soc. London, Spec. Publ.* 156, 295–334.

Gedl P. 2000: Palaeography of the Podhale Flysch (Oligocene, Central Carpathians, Poland) — its relation to the neighbourhood areas as based on palynological studies. *Slovak Geol. Mag.* 2–3, 150–154.

Golonka J., Krobicki M., Oszczypko N. & Ślączka A. 2005: Palinspastic modelling and Carpathian Phanerozoic palaeogeographic maps. In: Oszczypko N., Uchman A. & Malata E. (Eds.): Palaeotectonic evolution of the Outer Carpathian and Pieniny Klippen Belt Basins. *Inst. Nauk Geol. Uniw. Jagielloń.*, Kraków, 19–43.

Gross P. 1973: On the character of the Choč-Subtatric fault. *Geol. Práce, Spr.* 61, 315–319 (in Slovak).

Gross P., Köhler E., Biely A., Franko O., Hanzel V., Hricko J., Kupco G., Papšová J., Priechodská Z., Szalaiová V., Snopková P., Stránska M., Vaškovský I. & Zbořil L. 1980: Geology of Liptovská Kotlina (Depression). *ŠGÚDŠ*, Bratislava, 1–236.

Gross P., Köhler E. & Samuel O. 1984: A new lithostratigraphical division of the Inner-Carpathian Paleogene. *Geol. Práce, Spr.* 81, 103–117 (in Slovak).

Gross P., Köhler E., Mello J., Halouzka R., Haško J. & Nagy A. 1993: Geology of Southern and Eastern Orava. *GÚDŠ*, Bratislava, 1–292 (in Slovak).

Jacko S. & Janočko J. 2000: Kinematic evolution of the Central-Carpathian Paleogene Basin in the Spišská Magura region (Slovakia). *Slovak Geol. Mag.* 6, 4, 409–418.

Janočko J. & Jacko S. 1999: Marginal and deep-sea deposits of Central Carpathians Palaeogene Basin, Spišská Magura region, Slovakia: implication for basin history. *Slovak Geol. Mag.* 4, 281–292.

Janočko J., Gross P., Buček S., Karoli S., Žec B., Rakús M., Potfaj M. & Halouzka R. 2000a: Geological map of the Spišská Magura Mts. 1 : 50,000. *ŠGÚDŠ*, Bratislava.

Janočko J., Gross P., Polák M., Potfaj M., Jacko S. Jun., Rakús M., Halouzka R., Jetel J., Petro Ľ., Kubeš P., Buček S., Köhler E., Siráňová Z., Zlínska A., Halásová E., Hamršmíd B., Karoli S., Žec B., Fejdiová O., Milička J., Boorová D. & Žecová K. 2000b: Explanation to geological map of the Spišská Magura Mts. 1 : 50,000. *ŠGÚDŠ*, Bratislava, 1–174.

Jurewicz E. 2005: Geodynamic evolution of Tatra Mts. and the Pieniny Klippen Belt (Western Carpathians): problems and comments. *Acta Geol. Pol.* 55, 3, 295–338.

Kázmer M., Dunkl I., Frisch W., Kuhlemenn J. & Ozsvárt P. 2003: The Palaeogene forearc basin of the Eastern Alps and Western Carpathians: subduction erosion and basin evolution. *J. Geol. Soc.* 160, 413–428.

Kępińska B. 1997: Geologic and geothermal model of the Podhale Basin. *Studia, Rozprawy, Monografie 48, Polska Akademia Nauk*, Krakow, 1–105 (in Polish).

Kováč M. 2000: Geodynamical, palaeogeographical and structural evolution of the Carpathian-Pannonian region during the Miocene: New sight on the Neogene basins of Slovakia. *VEDA*, Bratislava, 1–202 (in Slovak).

Kováč M., Nagymarosy A., Soták J. & Šútovská K. 1993: Late Tertiary paleogeographic evolution of the Western Carpathians. *Tectonophysics* 226, 401–416.

Kováč M., Kráľ J., Márton E., Plašienka D. & Uher P. 1994: Alpine uplift history of the Central Western Carpathians: geochronological, paleomagnetic, sedimentary and structural data. *Geol. Carpathica* 45, 83–96.

Kováč P. & Hók J. 1996: Tertiary development of the western part of the Pieniny Klippen Belt. *Slovak Geol. Mag.* 2, 137–149.

Kráľ J. 1977: Fission track ages of apatite from some granitoids rocks in West Carpathians. *Geol. Zbor. Geol. Carpath.* 45, 83–96.

Maerten L. 2000: Variation in slip on intersecting normal faults: Implications for paleostress inversion. *J. Geophys. Res.* 105(B11), 25553–25565.

Maheľ M. 1986: Geological structure of the Czechoslovak Carpathians. Part 1. *VEDA*, Bratislava, 1–503 (in Slovak).

Marko F., Vojtko R., Plašienka D., Sliva Ľ., Jablonský J., Reichwalder P. & Starek D. 2005: A contribution to the tectonics of the Periklippen zone near Zázrivá (Western Carpathians). *Slovak Geol. Mag.* 11, 37–43.

Marko F., Vojtko R., Preusser F. & Madarás J. 2008: An attempt to date neotectonic faulting (Vikartovce fault, Western Carpathians). *Miner. Slovaca — Geovestník* 2, 242–243.

Marschalko R. & Radomski A. 1970: Sedimentary structures and marginal facies of the Eocene flysch near Ždiar. *Geol. Práce, Spr.* 53, 85–99.

Marshak S. & Mitra G. 1988: Basic methods of structural geology. *Prentice-Hall*, New Jersey, 1–446.

Márton E., Mastella L. & Tokarski A.K. 1999: Large counterclockwise rotation of the Inner West Carpathian Paleogene Flysch — evidence from paleomagnetic investigations of the Podhale Flysch (Poland). *Phys. Chem. Earth (A)*, 24, 8, 645–649.

Mastella L. 1975: Flysch tectonics in the eastern part of the Podhale Basin (Carpathians, Poland). *Rocz. Pol. Tow. Geol.* XLV, 3–4, 361–401.

Mastella L., Konon A. & Mardal T. 1996: Tectonics of the Podhale Flysh Basin in the Białka Valley. *Przegl. Geol.* 12, 1189–1194.

Michael A.J. 1984: Determination of stress from slip data: faults and folds. *J. Geophys. Res.* 89, B13, 11517–11526.

Müller B., Reinecker J. & Fuchs K. 2000: The 2000 release of the World Stress Map. World Wide Web address: http://www.world-stress-map.org

Nemčok J., Bezák V., Janák M., Kahan Š., Ryka W., Kohút M., Lehotský I., Wieczorek J., Zelman J., Mello J., Halouzka R., Raczkowski W. & Reichwalder P. 1993: Explanation to geological map of the Tatra Mts. 1 : 50,000. *GÚDŠ*, Bratislava, 1–135 (in Slovak).

Nemčok J., Bezák V., Biely A., Gorek A., Gross P., Halouzka R., Janák M., Kahan Š., Kotański Z., Lefeld J., Mello J., Reichwalder P., Raczkowski W., Roniewicz P., Ryka W., Wieczorek J. & Zelman J. 1994: Geological map of the Tatra Mountains. *MŽP SR, GÚDŠ*, Bratislava.

Nieto-Samaniego A.F. & Alaniz-Alvarez S.A. 1996: Origin and tectonic interpretation of multiple fault patterns. *Tectonophysics* 270, 197–206.

Olszewska B. & Wieczorek J. 1998: The Palaeogene of the Podhale basin (Polish Inner Carpathians) — micropalaeontological perspective. *Przegl. Geol.* 46, 8, 721–728.

Oszczypko N. 1992: Late Cretaceous through Paleogene evolution of Magura Basin. *Geol. Carpathica* 43, 6, 333–338.

Oszczypko N. 1998: The Western Carpathian Foredeep—development of the foreland basin in front of the accretionary wedge and its burial history (Poland). *Geol. Carpathica* 49, 6, 415–431.

Oszczypko N. & Ślączka A. 1989: The evolution of the Miocene basin in the Polish Outer Carpathians and their foreland. *Geol. Zbor. Geol. Carpath.* 40, 1, 23–37.

Oszczypko N., Oszczypko-Clowes M., Golonka J. & Marko F. 2005: Oligocene–Lower Miocene sequences of the Pieniny Klippen Belt and adjacent Magura nappe between Jarabina and Poprad River (East Slovakia and South Poland — their tectonic position and paleogeographic implications). *Geol. Quart.* 49, 379–402.

Oszczypko-Clowes M. & Oszczypko N. 2005: The position and age of the youngest deposits in the Mszana Dolna and Szczawa tectonic windows (Magura Nappe, Western Carpathians, Poland). *Acta Geol. Pol.* 54, 3, 339–367.

Pešková I., Vojtko R., Starek D. & Sliva Ľ. 2009: Late Eocene to Quaternary deformation and stress field evolution of the Orava region (Western Carpathians). *Acta Geol. Pol.* 59, 1, 73–91.

Plašienka D. 1999: Tectonochronology and paleotectonic model of the Jurassic–Cretaceous evolution of the Central Western Carpathians. *VEDA*, Bratislava, 1–125 (in Slovak with English summary).

Plašienka D. 2003: Dynamics of Mesozoic pre-orogenic rifting in the Western Carpathians. *Mitt. Österr. Geol. Gesell.* 94, 2001, 79–98.

Plašienka D. & Jurewicz E. 2006: Tectonic evolution of the Pieniny Klippen Belt and its structural relationships to the External and Central Western Carpathians. *Geolines* 20, 106–108.

Plašienka D., Grecula P., Putiš M., Kováč M. & Hovorka D. 1997: Evolution and structure of the Western Carpathians: an overview. In*:* Grecula P., Hovorka D. & Putiš M. (Eds.): Geological evolution of the Western Carpathians. *Miner. Slovaca — Monography,* Bratislava, 1–24.

Plašienka D., Soták J. & Prokešová R. 1998: Structural profiles across the Šambron-Kamenica Periklippen Zone of the Central Carpathian Paleogene Basin in NE Slovakia. *Miner. Slovaca* 30, 173–184.

Plašienka D., Vojtko R., Bučová J. & Mikuš V. 2007: The Pieniny Klippen Belt (Western Carpathians) — a former shallow fold-thrust belt affected by transpression. *Alpine Workshop 2007, Swiss Academy of Sciences*, Davos, 1–63.

Pollard D.D., Saltzer S.D. & Rubin A.M. 1993: Stress inversion method: are they based on faulty assumptions? *J. Struct. Geol.* 15, 8, 1045–1054.

Ramsay J.G. 1967: Folding and fracturing of rocks. *Mc Graw Hill*, New York, 1–568.

Ramsay J.G. & Huber M.I. 1987: The techniques of modern structural geology. 2: Fold and fractures. *Academic Press*, London, 1–700.

Ratschbacher L., Frisch W., Linzer H., Sperner B., Meschede M., Decker K., Nemčok M., Nemčok J. & Grygar R. 1993: The Pieniny Klippen Belt in the Western Carpathians of northeastern Slovakia: structural evidence for transpression. *Tectonophysics* 226, 471–483.

Roberts G.P. & Ganas A. 2000: Fault-slip directions in central and southern Greece measured from striated and corrugated fault planes: Comparison with focal mechanism and geodetic data. *J. Geophys. Res.* 105(B10), 23443–23462.

Royden L.H. & Báldi T. 1988: Early Cenozoic tectonics and paleogeography of the Pannonian Basin and surrounding regions. *Amer. Assoc. Petrol. Geol.*, *Mem.* 45, 1–16.

Sliva Ľ. 2005: Sedimentary facies of the Central Carpathians Palaeogene Basin in the area of Spišská Magura Mts. *PhD Thesis*, *Comenius University*, Bratislava, 1–137 (in Slovak).

Soták J. & Starek D. 2000: Synorogenic deposition of turbidite fans in the Central-Carpathian Paleogene Basin: evidence for and against sea-level and climatic changes. *Slovak Geol. Mag.* 6, 2–3, 191–194.

Soták J., Pereszlenyi M., Marschalko R., Milička J. & Starek D. 2001: Sedimentology and hydrocarbon habitat of the submarine fan deposits of the Central Carpathians Palaeogene Basin (NE Slovakia). *Mar. Petrol. Geol.* 18, 87–114.

Sperner B. 1996: Computer programs for the kinematic analysis of brittle deformation structures and the Tertiary tectonic evolution of the Western Carpathians (Slovakia). *PhD Thesis*, *Tübinger Geowiss. Arbeiten* A27, 1–120.

Sperner B., Ratschbacher L. & Nemčok M. 2002: Interplay between subduction retreat and lateral extrusion: Tectonics of the Western Carpathians. *Tectonics* 21, 6, 1051. doi:10.1029/2001TC901028.

Sperner B., Müller B., Heidbach O., Delvaux D., Reinecker J. & Fuchs K. 2003: Tectonic stress of the Earth's crust: advances in the World Stress Map Project. In: Nieuwland D.A. (Ed.): New insights in structural interpretation and modelling. *Geol. Soc. London, Spec. Publ.* 212, 101–128.

Tari G., Báldi T. & Báldi-Beke M. 1993: Paleogene retroarc flexural basin beneath the Neogene Pannonian Basin: a geodynamic model. *Tectonophysics* 226, 433–456.

Twiss R.J. & Unruh J.R. 1998: Analysis of fault slip inversions: Do they constrain stress or strain rate? *J. Geophys. Res.* 101, 8335–8361.

Vojtko R. 2003: Structural analysis of faults and geodynamic evolution of the central part of the Slovenské rudohorie Mts. *Manuscript, PhD Thesis*, *Comenius University*, Bratislava, 1–91 (in Slovak).

Vojtko R., Marko F., Madarás J., Beták J. & Preusser F. 2009: New evidence of neotectonic activity of the Vikartovce fault (Western Carpathians). *Tectonics and sedimentation, Conference Volume*, Bonn, 1–80.

Wagreich M. 1995: Subduction tectonic erosion and Late Cretaceous subsidence along the northern Austroalpine margin (Eastern Alps, Austria). *Tectonophysics* 242, 63–78.

Wallbrecher E. 1986: Tektonische und gefügeanalytische Arbeitsweisen. *Enke*, Stuttgart, 1–244.

Watycha L. 1959: Remarks on geology of the Podhale Flysch in the eastern part of Podhale. *Przegl. Geol.* 8, V, 350–356 (in Polish).

Westwalewicz-Mogilska E. 1986: New perspective on genesis of the Podhale flysch sediments. *Przegl. Geol.* 12, 690–698.

Winkler W. & Ślączka A. 1992: Sediment dispersal and provenance in the Silesian, Dukla, and Magura flysch nappes (Outer Carpathians, Poland). *Geol. Rdsch.* 81, 2, 371–382.

Zoback M.L. 1992: First- and second-order pattern of stress in the lithosphere: The World Stress Map Project. *J. Geophys. Res.* 97, 11703–11728.

Zuchiewicz W. 1995: Time-series analysis of river bed gradients in the Polish Carpathians: a statistical approach to the studies on young tectonic activity. *Z. Geomorphol.* 39, 4, 461–477.

Zuchiewicz W. 1998: Cenozoic stress field and jointing in the Outer West Carpathians, Poland. *J. Geodynamics* 26, 1, 57–68.